

Short communication

THE DIELECTRIC FUNCTION OF NaCl FROM LOW SCATTERING
ANGLE ELECTRON ENERGY-LOSS SPECTROSCOPY

RAUL A. ABREU

Centro de Fisica, IVIC, Apartado 1827, Caracas 1010A (Venezuela)

(First received 20 December 1983; in final form 15 June 1984)

Measurements of the electron energy-loss spectrum of NaCl have been reported [1], but no calculation seems to have been made of the wavevector dependence of its dielectric function. The purpose of this paper is to comment on some of the features of the dielectric function and the optical joint density of states function of NaCl deduced from new wavevector and energy-dependent energy-loss experiments.

Polycrystalline samples of NaCl were prepared by evaporation onto Formvar (polyvinyl formal) substrates under a conventional vacuum. Film thicknesses, estimated at about 500 Å, were of the order of the mean free path for volume excitations. A transmission energy-loss spectrometer, built around the frame of an EM3A electron microscope [2], was modified [3] for the recording of the high resolution measurements reported here. The energy resolution was between 0.1 and 0.3 eV, the poorer value corresponding to the highest scattering angle; the wavevector (scattering angle) resolution was 0.016 Å⁻¹ (0.15 mrad).

Room temperature transmission energy-loss spectra were recorded with 45 keV electrons in the 0–50 eV region, and at various scattering angles covering momentum transfers of up to 0.145 of the Γ X Brillouin zone dimension. The dielectric function $\epsilon(k, \omega) = \epsilon_1(k, \omega) + i\epsilon_2(k, \omega)$ was calculated from the energy-loss spectra through Kramers–Krönig analysis [4] and scaled in the long wavelength limit, where $\epsilon_2 = 0$, to the known refractive index of NaCl, $n = \sqrt{\epsilon_1} = 1.54$. Figure 1 shows the energy dependence of the dielectric function for four different values of k . It is useful to evaluate the optical joint density of states function $J(\omega)$, defined as

$$J(\omega) = \left(\frac{m}{2\pi^2 e^2 N} \right) \omega \epsilon_2(\omega) \quad (1)$$

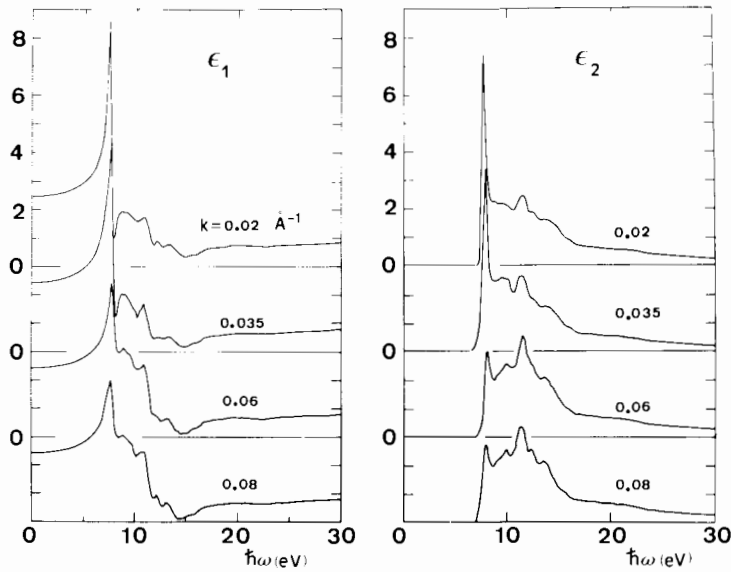


Fig. 1. Energy dependence of the real (ϵ_1) and imaginary (ϵ_2) parts of the dielectric function of NaCl deduced from energy-loss spectra recorded at 0.20, 0.32, 0.55, and 0.75 mrad, corresponding to k -transfers of 0.02, 0.035, 0.06, and 0.08 \AA^{-1} , and representing the fractions 0.036, 0.063, 0.11, and 0.145 of the Γ X Brillouin zone dimension.

and has units of states per unit cell per unit frequency, where e and m are the electron charge and mass, and N is the number of unit cells per unit volume. It is possible, under certain conditions [5], to associate $J(\omega)$ with the joint density of states function. The integral of $J(\omega)$, evaluated up to the experimental upper frequency limit, leads to

$$n(\omega) = \int_0^{\omega} J(\Omega) d\Omega = \frac{m}{2\pi^2 e^2 N} \int_0^{\omega} \Omega \epsilon_2(\Omega) d\Omega \quad (2)$$

where $n(\omega)$ gives the effective number of electrons that take part in transitions up to the energy $\hbar\omega$. Figure 2 shows $J(\omega)$ and $n(\omega)$ calculated from the energy-loss spectrum recorded at 0.2 mrad, corresponding to the lowest k -transfer reported here (0.02 \AA^{-1}).

Existing band structure calculations [6–8] and optical measurements [9] are used in the assignment of structures in $J(\omega)$. The valence band originates from the highest filled $3p$ states of Cl^- . The corresponding wave function is very localized on the Cl^- ion sites and has strong p -character. The spin orbit splitting at Γ gives rise to doubly degenerate states ($j = \frac{1}{2}, \frac{3}{2}$) at the top, and a non-degenerate state at a lower energy. The degeneracy is removed at points of lower symmetry, resulting in three non-degenerate states. The

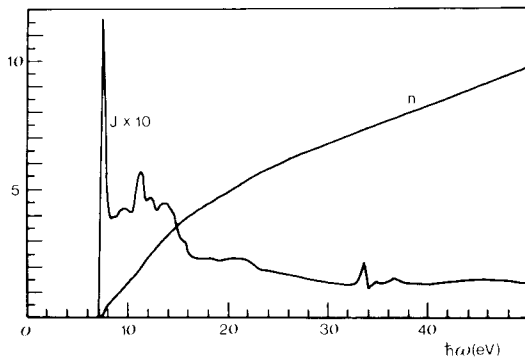


Fig. 2. Optical joint density of states function $J(\omega)$ and effective number of electrons $n(\omega)$ calculated from the energy-loss spectrum recorded at 0.20 mrad.

valence band has maxima at Γ_{15} , L_3 , and X_5' . The conduction band has an absolute minimum at Γ_1 ; the wave function is mainly s -like at this point [10]. Away from Γ , conduction band minima are found at X_1 , X_3 , and L_1 . The d -levels at X_3 are not a well-defined minimum [7], and are thought to be degenerate with the s -level at X_1 [6].

A summary of the major $J(\omega)$ and $\epsilon_2(\omega)$ peak positions deduced from the $k = 0.02 \text{ \AA}^{-1}$ energy-loss spectrum is shown in Table 1, along with related results from near-normal incidence reflectivity [9] and optical absorption [11] experiments, and from band structure calculations [6, 8]. The agreement with the optical results is, in most cases, within the resolution limit of the present experiments. The first strong peak in $J(\omega)$ at 7.19 eV, and the following weak structure at 8.66 eV, are identified as the first two members of a Wannier-type exciton series at Γ . The spin orbit splitting of the valence band is too small to be observed at room temperature. The energy gap is at a higher energy, and the 8.97 eV estimate of ref. 9 seems reasonable. The following four peaks in $J(\omega)$ are assigned to interband transitions at Γ , X and L , as indicated in Table 1. The best agreement is with a recent self-consistent APW- $k.p$ band structure calculation [8]. The structures above 15 eV arise from transitions to higher conduction band levels, judging from the strong decrease in $J(\omega)$ in that region and the weakness of the observed features.

The peak at 33.6 eV marks the onset of the excitations from the $\text{Na}^+ 2p$ level, and is known as a core exciton, which has a large oscillator strength compared with other absorption bands in the region [11]. The assignment of the following small peaks at 34.8 and 36.7 eV is speculative. It is proposed that these are due to transitions from the $2p$ level to the conduction band at L_2' and X_1 , respectively. This assignment is made assuming that these two peaks are due to transitions to the same conduction band states as in the

TABLE 1
 MAJOR $J(\omega)$ AND $\epsilon_2(\omega)$ PEAK POSITIONS (eV) FOR $k = 0.02 \text{ \AA}^{-1}$, AND COMPARISON WITH PUBLISHED DATA AND BAND STRUCTURE CALCULATIONS

This work		Published data		Band transition	Band structure calculations	
$J(\omega)$	$\epsilon_2(\omega)$	$\epsilon_2(\omega)^a$	Absorption ^b		S.c. APW- $k.p$ ^c	Mixed-basis ^d
—	—			$\Gamma_{15} \rightarrow \Gamma_1$ gap	6.90	10.0
7.19	7.6	7.75		Γ exciton	—	—
8.66	8.75	(8.6) ^e		Γ exciton ($n = 2$)	—	—
9.63	9.4	10.0		$L_3 \rightarrow L_2'$	9.42	12.7
11.22	11.4	11.2		$X_5' \rightarrow X_1$	10.2	14.2
12.32	12.2	12.3		$X_5' \rightarrow X_3$	10.5	14.2
13.78	13.4	13.5		$L_3 \rightarrow L_3'$	13.1	17.3
—	—			$\Gamma_{15} \rightarrow \Gamma_{25}$	13.0	17.6
33.6	33.6		33.5	$\text{Na}^+ 2p$ Γ exciton		
34.8	34.8		34.75	$\text{Na}^+ 2p \rightarrow L_2'$		
36.7	36.7		36.6	$\text{Na}^+ 2p \rightarrow X_1$		

^a Calculated from optical reflectivity [9].

^b Optical absorption data [11].

^c Self-consistent APW- $k.p$ band structure calculation [8].

^d Nonrelativistic mixed-basis band structure calculation [6].

^e Weak structure at room temperature [9].

case of the first two strong interband peaks at 9.63 and 11.22 eV. The energy separation between the exciton and the following two peaks is greater in the interband region than in the $2p$ level region due to the greater curvature of the valence band.

Some dispersive effects are evident from the $\epsilon_2(\omega)$ curves of Fig. 1. The major change corresponds to the Γ exciton peak, which decreases in intensity and moves to higher energies with increasing scattering angle, from 7.6 eV at 0.2 mrad to 8.0 eV at 0.75 mrad. No change in position is observed in the rest of the interband peaks that are stronger towards high scattering angles modifying the overall ϵ_2 lineshape.

ACKNOWLEDGEMENTS

The experiments were performed at the Cavendish Laboratory, Cambridge University. The author is grateful to W.Y. Liang and A.D. Yoffe for their support throughout the course of this work.

REFERENCES

- 1 M. Creuzburg, *Z. Phys.*, 196 (1966) 433.
- 2 M.G. Bell and W.Y. Liang, *Adv. Phys.*, 25 (1976) 53.
- 3 R.A. Abreu, Ph.D. Thesis, Cambridge University, 1977.
- 4 J. Daniels, C. Festenberg, H. Raether and K. Zeppenfeld, *Springer Tracts Mod. Phys.*, 54 (1970) 77.
- 5 W.Y. Liang and A.R. Beal, *J. Phys. C*, 9 (1976) 2823.
- 6 N.O. Lipari and A.B. Kunz, *Phys. Rev. B*, 3 (1971) 491.
- 7 F. Bassani and E.S. Giuliano, *Nuovo Cimento B*, 8 (1972) 193.
- 8 I.C. da Cunha Lima, A. Ferreira da Silva and N.J. Parada, *Int. J. Quantum Chem.*, 20 (1981) 933.
- 9 D.M. Roessler and W.C. Walker, *Phys. Rev.*, 166 (1968) 599.
- 10 G. Baldini and B. Bosacchi, *Phys. Rev.*, 166 (1968) 863.
- 11 S. Nakai, T. Ishii and T. Sagawa, *J. Phys. Soc. Jpn*, 30 (1971) 428.